SUPPLEMENTARY MATERIAL

The following sections aim to integrate the analyses included in the manuscript *"Intervention strategies for the seismic improvement of masonry buildings based on FME validation: the case of a terraced building struck by the 2016 Central Italy earthquake" by M.R. Valluzzi *, L. Sbrogiò, Y. Saretta,* submitted to Buildings MDPI on July 2021.

Procedure for model calibration basing on damage analysis

The calibration procedure exploits the seismic damage pattern as the phenomenological representation of a building's behaviour in the complex dynamic conditions of an earthquake. An appropriate interpretation of these patterns can guide modelling choices so that the model's behaviour matches at best that of the actual building. The calibration is done by varying the possible input parameters, e.g., those accounting for mechanical properties of (a) masonry walls, (b) connections and, (c) floor slabs, and monitoring output ones. These output parameters may vary according to the modelling approach and the target of calibration: the former condition reflects on the type of output (e.g., tensile strain in finite element modelling or rotation of plastic hinges in equivalent frame approach) and the latter on the type of structural parameter considered (e.g., modal frequencies in operational modal analysis or damage state, as in this case). The process ends when the best match between the numerical representation and the actual value of the parameter is obtained. In this work, the monitored parameter was the damage state reached at the conclusion of non-linear static analyses in 3Muri software, as determined by comparison with strength domains of each masonry element. The calibration process was carried out on unit no. 6 of the IACP building (refer to Figures 4, 8b and 9a in the main manuscript), i.e., the most damaged, and its results were then extended to the whole complex.

(a) Mechanical properties of masonry piers

The mechanical properties of the case study's masonry were obtained indirectly, that is by considering only the visual quality of the building material, though within the framework of the so-called 'masonry quality method' [S1], and then by matching it to the reference types provided by technical codes [S2]. This was valid for the stone masonry of the case study, which was used in the piers, whereas the spandrels' block masonry (a common type used in the middle 20th century, although non-standard, i.e., with holes parallel to bed joints) fell outside the limits of current codes. Therefore, for this latter, mechanical properties were inferred from experimental campaigns on similar materials [S3]. Notwithstanding, the code allows a minimum additional variability, to consider a masonry's peculiar conditions (e.g., very good or very poor preservation state). The evaluation of masonry quality revealed that stone masonry, though with a different external pattern, shared the absence of bond stones and a cross section subdivided in two leaves, with widespread voids. In addition, the piers suffered of heavy diagonal shear damage, which was considered an evidence of scarce mechanical properties, whilst the spandrels showed just slight flexural damage. The parametrical variations considered the following cases:

- 1a – cracked stiffness on each material;
- 1b – cracked stiffness on stone masonry only;
- 1c – poor masonry condition on each material;
- 1d – poor masonry and cracked stiffness on each material;
- 1e – poor masonry on each material and cracked stiffness on stone masonry only.

The cracked stiffness is commonly quantified in a reduction to half of the material's stiffness, to consider the damage, and the consequent reduction in seismic forces suffered by a building. According to the Italian seismic code, a poor masonry condition implies a reduction to the 80% and to the 70% of elastic and strength properties, respectively; other parameters were assumed as cases '2d' and '3d' in the following sections.

**Corresponding author: M.R. Valluzzi (mariarosa.valluzzi@unipd.it)*

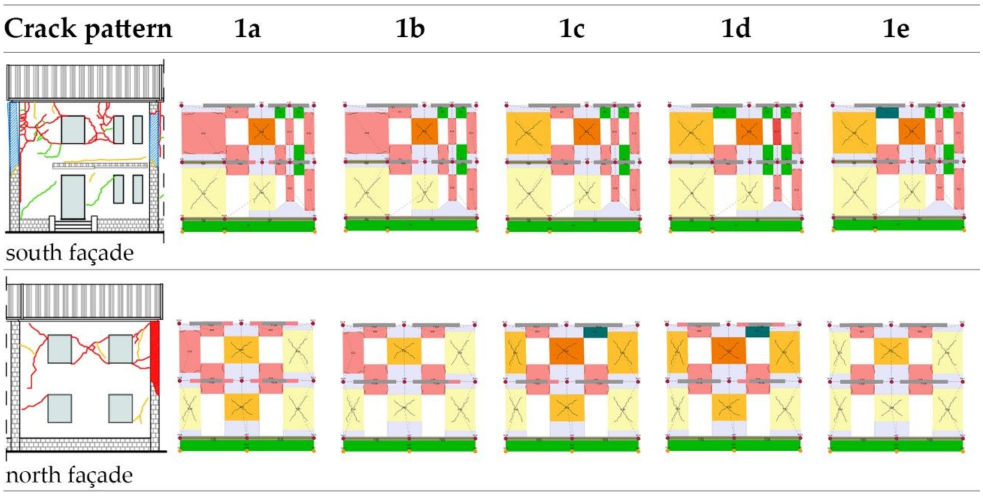

Figure S1. Observed crack pattern and numerical damage state of models with parametrical variations of masonry properties on unit no. 6 (see Figure 4 in main manuscript).

The decrease of masonry properties, especially the shear strength, allowed a better match of the numerical damage state of piers with the observed crack pattern, as flexural failure (Figure S1, cases 1a and 1b) changed into diagonal shear (Figure S1, cases '1c' and '1d'). The influence of stiffness properties on damage state was negligible (Figure S1, cases '1d' and '1e').

(b) Coupling of piers

In 3Muri, the coupling among piers belonging to the same wall is governed by: i) the diaphragms' stiffness in the direction parallel to the wall; ii) the tensile-resistant elements (tie beams, tie rods) in spandrels; iii) the shear/tensile strength of the material which spandrels are composed of. Therefore, the parametrical analyses considered the following cases:

- 2a – no coupling (null parallel stiffness, no tie beams/tie rods);
- 2b – diaphragm coupling (finite parallel stiffness, no tie beams/tie rods);
- 2c – coupling devices (tie beams/tie rods, null parallel stiffness);
- 2d – coupling devices and diaphragm coupling (tie beams/tie rods and finite parallel stiffness);
- 2e – shear strength of the material of spandrels, with the following subcases: i) a half of the reference value; ii) the reference value; iii) 1.5 times the reference value.

The connecting devices were simulated by tie beams with a 25x12 cm cross section (base, height) and minimum amount of longitudinal (4Ø10) and transverse reinforcement (Ø6 @ 50 cm); therefore, just the additional tensile strength of rebars was considered. The reference value of the spandrels' shear strength, as defined by [S3] is 0.09 MPa. Other parameters were fixed at those of model '1d' and '3d'.

The absence of connecting devices at floor levels determined both a heavy damage in piers and a prevalence of flexure on diagonal shear ('weak spandrel' behaviour), which did not match with the actual crack pattern (Figure S2, '2a' and '2b'). Once spandrels expressed some tensile strength, through steel elements, the damage state shifted to diagonal shear ('strong spandrel' behaviour, Figure S2, '2c') but an additional coupling by the means of floor stiffness was required to reach a proper level of damage (Figure S2, '2d'). The variation of the spandrel's shear strength only reflected on their damage state, which actually was a flexural one or negligible: the reference value or higher resulted in the desired behaviour (Figure S3, '2e-ii' and '2e-iii'), whereas the reduction to half its value caused shear damage (Figure S3, '2e-I').

*Corresponding author: M.R. Valluzzi (mariarosa.valluzzi@unipd.it)

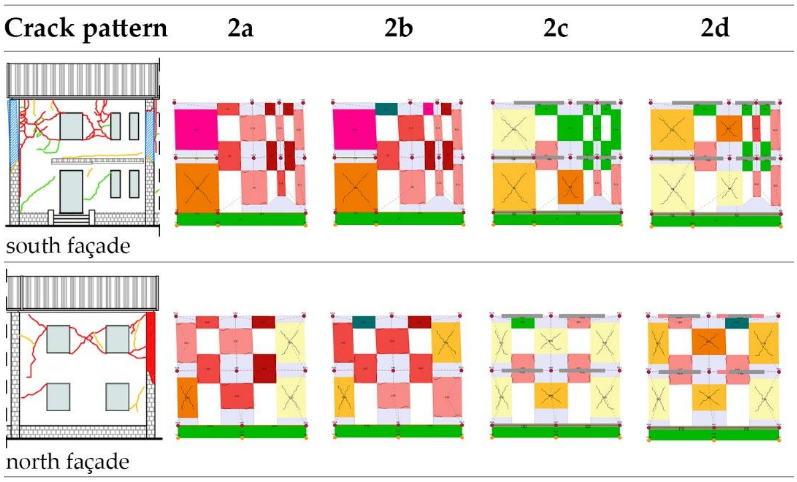

Figure S2. Observed crack pattern and numerical damage state of models with parametrical variations of coupling among piers on unit no. 6 (see Figure 4 in main manuscript).

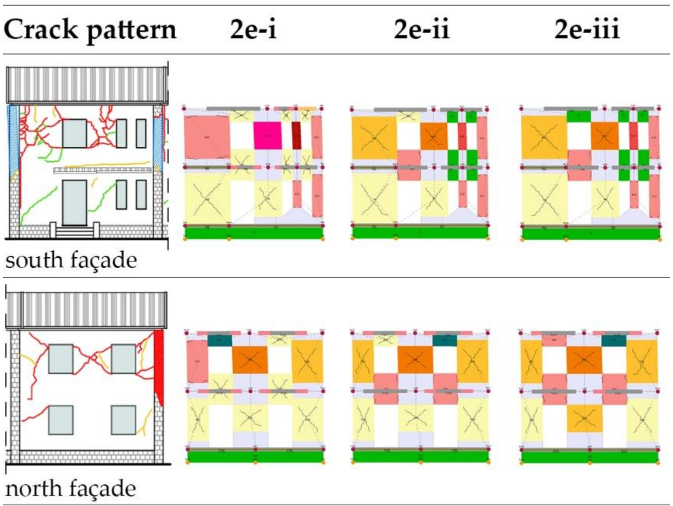

Figure S3. Observed crack pattern and numerical damage state of models with parametrical variations of spandrel's shear strength on unit no. 6 (see Figure 4 in main manuscript).

(c) Diaphragm stiffness

Diaphragm stiffness was expressed by two Young's moduli in the two main directions of the membrane E_1, E_2 (subscript 1 refers to the direction of the floor span and subscript 2 to that orthogonal to it) and the shear modulus G_{12} between them. The elastic moduli account for the coupling of piers belonging to the same wall, as they provide a link between the nodes of a wall and therefore govern forces on spandrels; the shear modulus governs the transfer of horizontal forces between orthogonal walls. The possible cases were explored as follows:

- 3a – infinite flexibility (null E and G);
- 3b – shear stiffness (null E, finite G);
- 3c – elastic stiffness (finite E, null G);
- 3d – shear and elastic stiffness (finite E ad G);
- 3e – rigid diaphragm (infinite E and G).

**Corresponding author: M.R. Valluzzi (mariarosa.valluzzi@unipd.it)*

The finite values of E and G account for the building's actual floor slab, which consists of clay joists reinforced by steel rebars. Therefore, the stiffness properties of the equivalent membrane were assumed as those of a clay block masonry: E_1=E_2=1200 MPa and G=300 MPa [S2]. It is worth noting that cases '2c' and '3c' coincide. The other parameters were fixed to the values of models '1d' and '2d'.

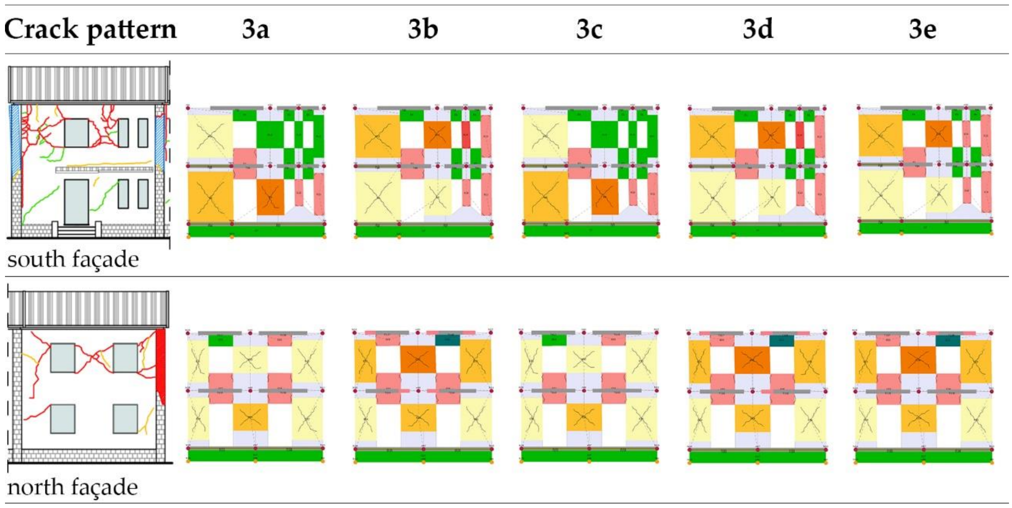

Figure S4. Observed crack pattern and numerical damage state of models with parametrical variations of diaphragm stiffness on unit no. 6 (see Figure 4 in main manuscript).

The comparison between the actual crack pattern and each damage state of the façade confirmed that floors slabs behaved as rigid in their plane and that shear stiffness was non-negligible. In facts, those models with at least finite values of G (Figure S4, '3b', '3d') showed a better match with the crack pattern than those with null G value (Figure S4, '3a', '3c'), especially at the first storey. In addition, almost no difference was detected in the damage states of the models with the finite and infinite values of G (Figure S4, '3d' and '3e').

Conclusions

The calibration process permitted to identify the set of parameters which best match with the observed damage patterns as: i) reduced mechanical properties of masonry owing to poor quality conditions and cracked stiffness; ii) moderate pier coupling through tie beams and iii) moderate in plane diaphragm stiffness. These properties correspond to those cases signed under the letter 'd' in each calibration stage, which was assumed as reference model to simulate various intervention scenarios and assess their performance as improvement seismic conditions for the case study in question.

References

[S1] Borri, A.; Corradi, M.; De Maria, A. The failure of masonry walls by disaggregation and the Masonry Quality Index. *Heritage* 2020, *3*, 1162-1198. https://doi.org/10.3390/heritage3040065.

[S2] MIT 2019, Ministry of Infrastructures and Transportations, Regulation n. 7/2019. Istruzioni per l'applicazione dell'Aggiornamento delle "Norme tecniche per le costruzioni" di cui al decreto ministeriale 17 gennaio 2018. Available online: https://www.gazzettaufficiale.it/eli/id/2019/02/11/19A00855/sg <https://www.gazzettaufficiale.it/eli/id/2019/02/11/19A00855/sg> (accessed on 30 June 2021). (in Italian)

[S3] Messali, F.; Metelli, G.; Plizzari, G. Experimental results on the retrofitting of hollow brick masonry walls with reinforced high performance mortar coatings. Constr Building Materials 2017, 141, 619–630, doi:10.1016/j.conbuildmat.2017.03.112.

Corresponding author: M.R. Valluzzi (mariarosa.valluzzi@unipd.it)